Paper

Sensitivity Calibration of UHF Partial Discharge Monitoring System in GIS

Member Tatsuro Kato (Hitachi, Ltd.)
Member Fumihiro Endo (Hitachi, Ltd.)
Member Shingo Hironaka (Hitachi Engineering & Service Co., Ltd)

Partial discharge (PD) monitoring system by UHF (Ultra high frequency) method has high sensitivity and high S/N ratio. This UHF PD monitoring system is suitable for PD diagnosis of GIS. Calibration technique of highly sensitive UHF sensor was clarified by injecting the artificial PD pulses. PD sensitivity of each sensor was verified and calibrated results were fully satisfactory. PDs were simultaneously measured with both the conventional method described in IEC-60270 and the UHF PD monitoring system by using many kinds of PD sources and various tank sizes. Owing to this measurement, conversion of dBm units in UHF PD monitoring system to pC units (apparent charge) became possible and it was clarified that the conversion curve was independent of PD sources and tank size. These characteristics were confirmed by the theoretical analysis.

Keywords : partial discharge, insulation diagnosis, UHF method, calibration, SF_6 gas, GIS

1. Introduction

Higher reliability is demanded with gas insulated apparatuses such as gas insulated switchgear (GIS) and gas insulated circuit breaker (GCB). Since gas insulated apparatuses are closed structure, it is difficult to find internal defects from outside. Therefore, development of a preventive maintenance technique is necessary for GIS to prevent failures and to detect defects early. Detection of PD is effective for these purposes [1]-[4]. PD signals in SF_6, especially, have a frequency component of high and wide bandwidth (UHF region), which is more than a few hundred MHz [5]-[8]. We have developed the UHF method diagnostic system which uses the neural network to improve the reliability of GIS [9].

UHF partial discharge monitoring system (UHF PDM) has become popular for PD diagnosis of GIS in recent years, and has been regulated as one of the PD measuring methods in IEC-60270. Many experiences were reported to clarify its performance [10, 11]. For accurate diagnosis, extremely high sensitivity of sensors and proper algorithms for PD assessment are necessary. Moreover, PD is measured in dBm units by UHF PDM, which is quite different from the conventional pC unit (apparent charge). The conversion between dBm and pC is demanded to help understanding of PD severity.

The present paper describes the sensitivity and calibration of UHF internal and external sensors. UHF PDM is experimentally compared with a conventional PD measuring system described in IEC 60270 and the obtained pC - dBm relationship is theoretically discussed.

2. Highly Sensitive UHF Sensor

High sensitivity UHF sensor is required to measure PD in detail by the UHF method. The UHF sensor used for this measurement is explained below.

2.1 Internal UHF Sensor The new internal UHF sensor consists of two half-disc plates [9]. Their size and arrangement were optimized based on dipole antenna technology. Sensitivity was greatly enhanced and directivity was negligible. Minute PD can be detected with this UHF sensor. Figure 1 shows examples measured in coaxial electrodes of 60/250 mm diameter. 3-mm long particle could be detected with sufficient intensity and S/N ratio even in the case where a particle was attached on a spacer. Sensitivity of the new UHF sensor was confirmed to be 0.3 pC (apparent charge) at S/N = 3 and 0.1 pC at S/N = 1 (Fig. 2). The dBm value was measured by spectrum analyzer. Signal Intensity dBm define the maximum amplitude of frequency region from 500 MHz to 1500 MHz. Noise level define the magnitude of back ground noise which consist of white noise of measuring apparatuses or external noise.

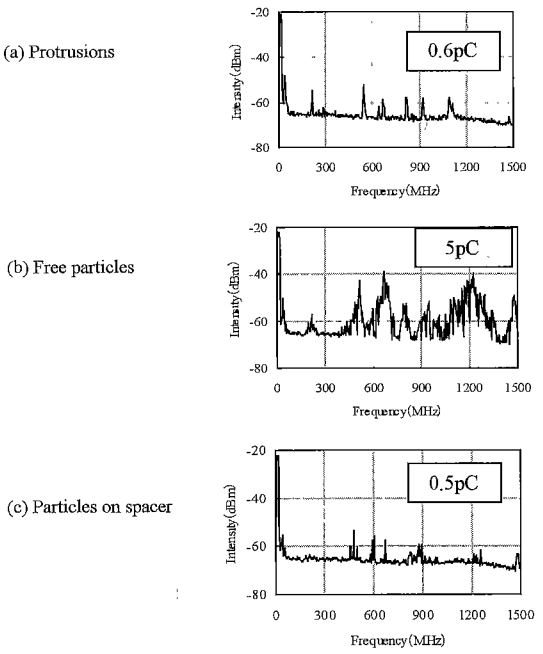

(particle: dia.=0.25mm, length=3mm, Inner dia. of tank=250mm, Outer dia. of cond.=60mm)

Fig. 1. Frequency spectra of PDs in 3 cases

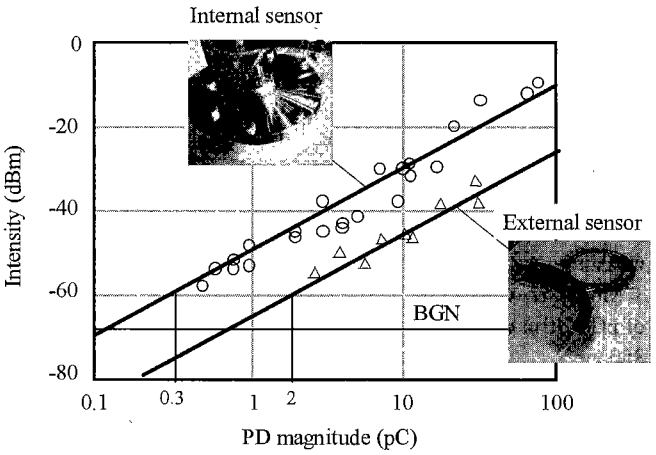

Fig. 2. Sensitivity of developed UHF sensor

The pC value was measured at the same time with a conventional method according to IEC-60270.

2.2 External UHF Sensor The external UHF sensor was designed to be fitted around the outer surface of a spacer. As part of UHF waves emitted from PDs leak through the outer edge of a spacer and its intensity is usually small, the structure of the sensor was designed based on the antenna theory to obtain high sensitivity. The developed sensor has the sensitivity of 2 pC at S/N = 3 (Fig. 2).

3. Sensitivity Verification

The artificial PD pulse for sensitivity calibration of the UHF sensor was described in the document CIGRE TF 15/33.03.05 [11]. Tests were performed with a bus model of 100/400 mm diameter (figure 3 (a)). The response characteristics of UHF sensors were measured by injecting the artificial PD pulse (the rise time: 0.5 ns, the time to half-value: 30 ns) from one UHF sensor and the value of the UHF signal was measured at the other sensor. The pulse magnitude was equivalent to an apparent charge of 5 pC. Fig. 3 (b) and (c) show the typical spectra measured with the internal and external sensors. PDs were generated at the vicinity of the sensor by using a 5-mm long particle, and the measured spectrum is shown in Fig. 3 (e). Equivalent spectra were obtained from 500 to 1500 MHz

Next, instead of the artificial PD pulse, a white noise (equivalent to an apparent charge of 5 pC) was injected from the tracking generator and the signal was measured. The near spectrum pattern was obtained (Fig. 3 (d)). This means that the white noise method is applicable for sensitivity verification.

Sensitivity evaluation of each UHF sensor of extra high-voltages GIS was performed using artificial pulses and white noise signals as outlined in Fig. 3 and show the maximum of each UHF sensor in Table 1. The variation in output value of a sensor is less than several dB, with all sensors being found normal after checking.

Moreover, the propagation characteristics of the electromagnetic waves between sensors were investigated. Since attenuation characteristics of GIS components is known, the total amount of attenuation can be calculated between sensors. We checked that the measured and calculated values of the amount of attenuation between sensors were in agreement. As it turned out, the same results were obtained and both can use artificial PD pulses and white noise signals for calibration of UHF sensors built in GIS.

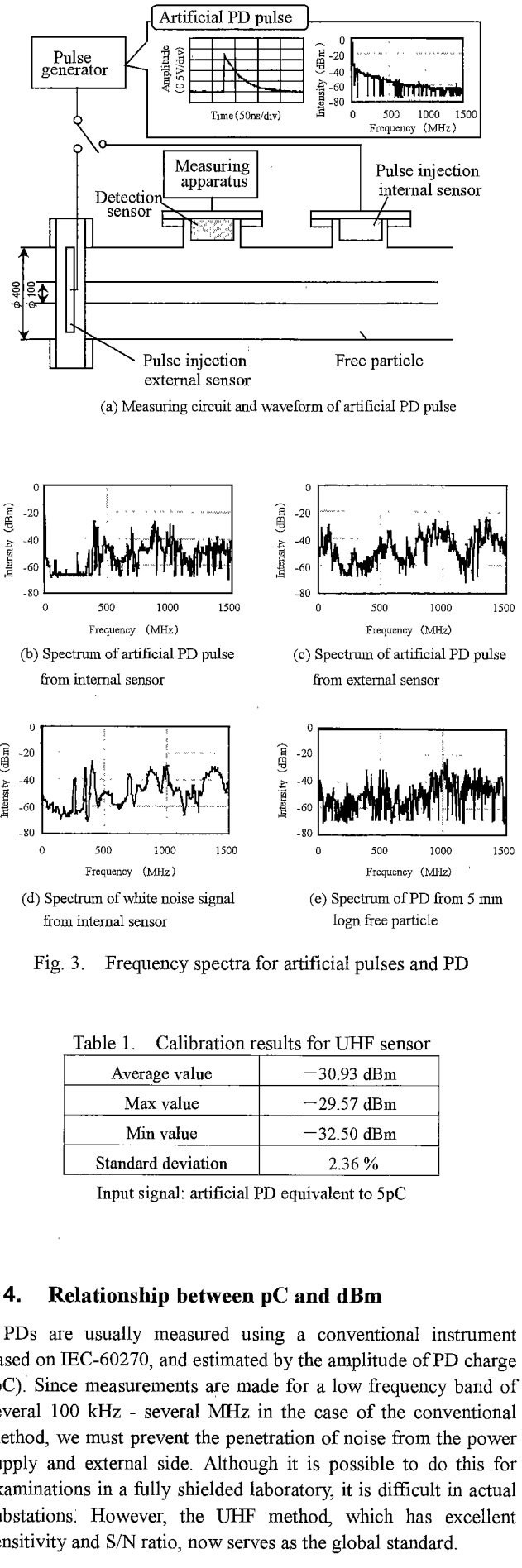

Fig. 3. Frequency spectra for artificial pulses and PD

Table 1. Calibration results for UHF sensor

Average value	−30.93 dBm
Max value	−29.57 dBm
Min value	−32.50 dBm
Standard deviation	2.36 %

Input signal: artificial PD equivalent to 5pC

4. Relationship between pC and dBm

PDs are usually measured using a conventional instrument based on IEC-60270, and estimated by the amplitude of PD charge (pC). Since measurements are made for a low frequency band of several 100 kHz - several MHz in the case of the conventional method, we must prevent the penetration of noise from the power supply and external side. Although it is possible to do this for examinations in a fully shielded laboratory, it is difficult in actual substations. However, the UHF method, which has excellent sensitivity and S/N ratio, now serves as the global standard.

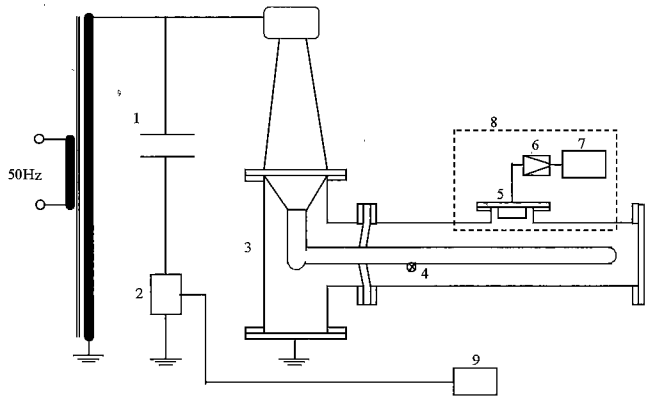

1: HV. Coupling Capacitor
2: Input Unit
3: SF_6 Test Chamber for PD
4: PD Source
5: UHF Sensor
6: Pre-Amplifier
7: Spectrum Analyzer
8: UHF PDM System
9: Discharge Detector

Fig. 4. Measuring circuit

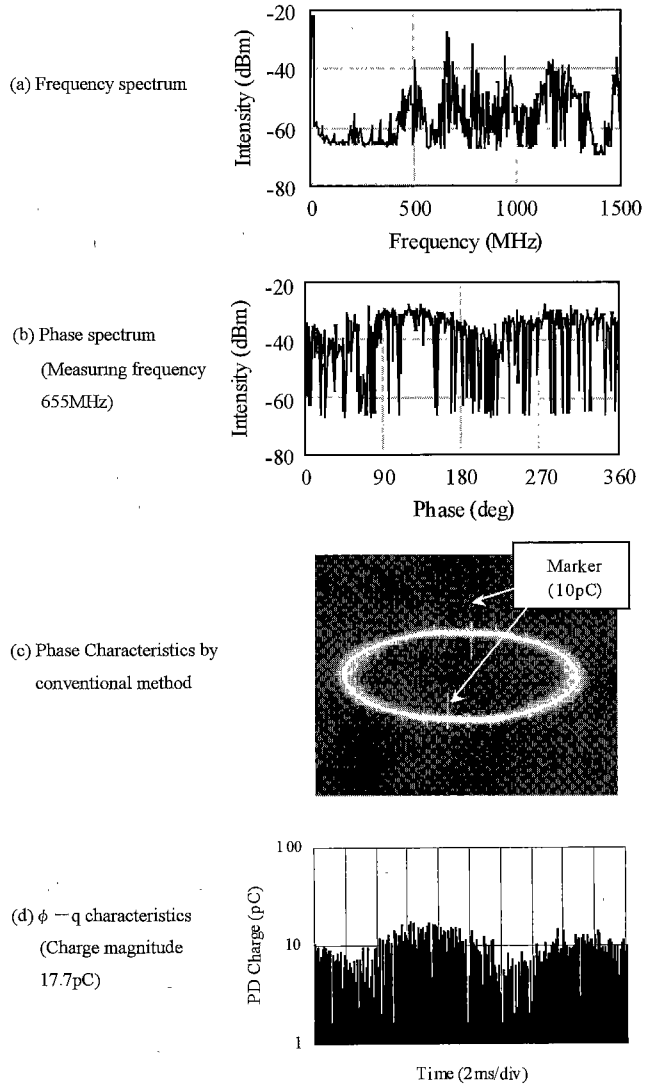

Fig. 5. Typical PD characteristics in free particle case

4.1 Experimental method Figure 4 shows the measuring circuit for pC - dBm conversion of PD magnitude. Various PD sources were placed in the coaxial cylinder electrodes of 60/250 mm diameter. Both the discharge detector by conventional instrument based on IEC-60270 and the UHF PDM system were connected to the calibration circuit. PD sources included protrusion, free metallic particle, particle on spacer, void in spacer, etc. PD signals were measured simultaneously by both measuring systems.

Moreover, we also investigated the tank diameter dependability of pC - dBm conversion with tank diameters in the range of 250 - 850 mm.

4.2 Experimental Results PDs were generated using typical PD sources in SF_6 insulation. PDs were measured simultaneously by both detectors. Figure 5 shows examples of measured results for free metallic particles. Figure 5 (a) and (b) show frequency spectrum and phase spectrum measured by UHF PDM system, and (c) and (d) show phase characteristics, and ϕ–q characteristics measured by the conventional system. Comparing (b) and (d), it can be observed that the phase characteristics are almost identical. In this case, the magnitude, q, of the PD pulse was 17.7 pC by the conventional method, and –27.6 dBm by the UHF PDM system.

Figure 6 shows examples of frequency and phase spectra for various defects. Here, we can observe which applied voltage phase PD generated the phase spectrum. In fact, results showed that the

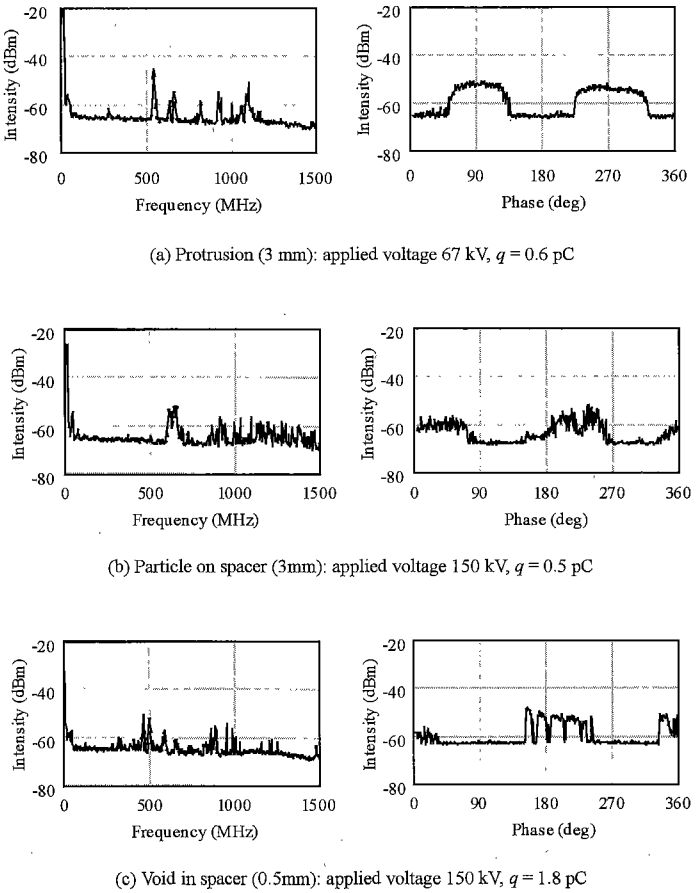

(a) Protrusion (3 mm): applied voltage 67 kV, q = 0.6 pC

(b) Particle on spacer (3mm): applied voltage 150 kV, q = 0.5 pC

(c) Void in spacer (0.5mm): applied voltage 150 kV, q = 1.8 pC

Fig. 6. Frequency and phase spectra for various defects

PD pattern was different for each defect. Since the output in the UHF method is measured in dB units, in order to judge the risk of defects, we must convert these units pC units currently used from the former. Figure 6 shows (a) –49 dBm at q = 0.6 pC, (b) –50 dBm at q = 0.5 pC, (c) –48 dBm at q = 1.8 pC. Thus, dBm values were calibrated as pC values for various defects. Figure 7 plots the magnitude q (pC) of PD charges by the conventional method and the maximum intensity (dBm) of 400 - 1500 MHz by the UHF method. In Fig. 7, a remarkable difference for various defects was not observed. Even for different kinds of defect, measured data converges well to a single curve. This curve can be expressed by equation (1).

$$q = 10^{(x+50)/20} \quad \cdots\cdots (1)$$

That is, pC is easily converted from the measured dBm value from equation (1).

Figure 8 shows pC - dBm characteristics of various tank sizes. It is clear that even if the tank size changes, the relationship between pC and dB converges well to a single curve. No dependency on tank size is observed. The relationship between pC and dBm can be expressed in equation (1).

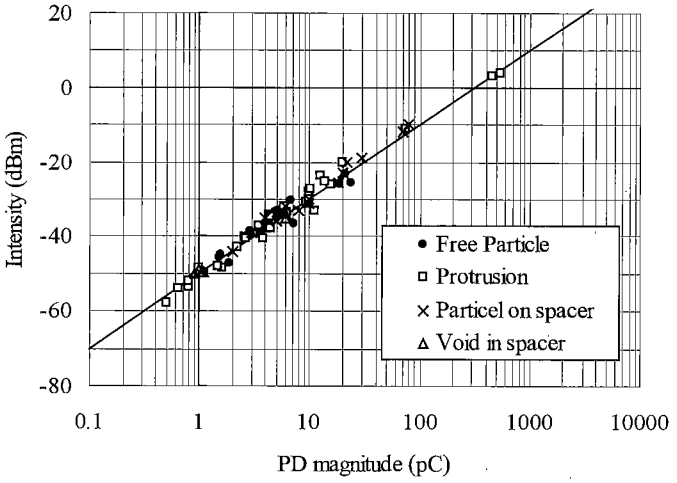

Fig. 7. pC - dBm characteristics for various defects

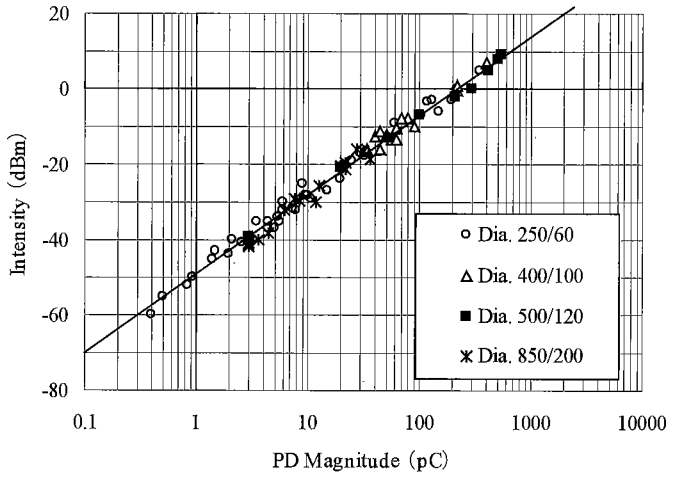

Fig. 8. pC - dBm characteristics for different tank size

4.3 Theoretical Analysis of dBm-pC Conversion PDs are generated in a minute space where electric field exceeds the discharge initiation field strength, and the real charge of PDs is determined by the capacitance of this minute space. However, the magnitude of real charge cannot be measured. Therefore, apparent charge q, which moves due to the capacitance between high voltage electrode and grounding electrode, is measured. Since the minute space is small sufficiently compared with the space between electrodes, q is inversely proportional to the tank diameter b [12]. Apparent charge, q,is expressed by the following equation.

$$q \propto 1/b \quad \cdots\cdots (2)$$

As the tank diameter increase, the apparent charge decreases, even if the real charge remains constant.

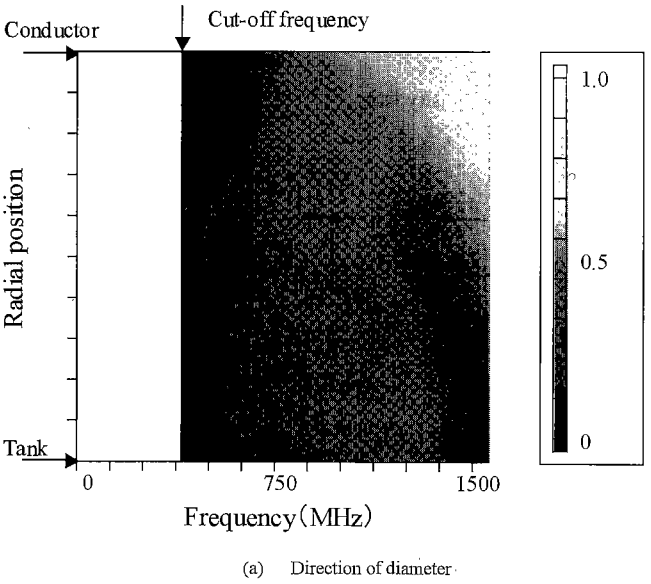

(a) Direction of diameter

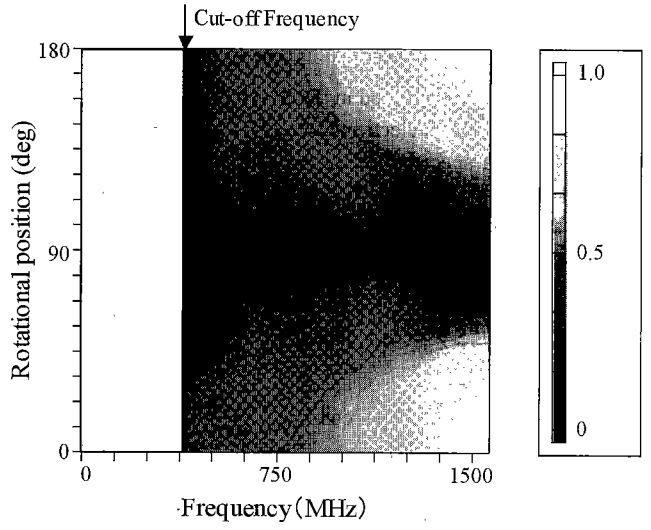

(b) Direction of rotation

Fig. 9. Electromagnetic distribution in tank

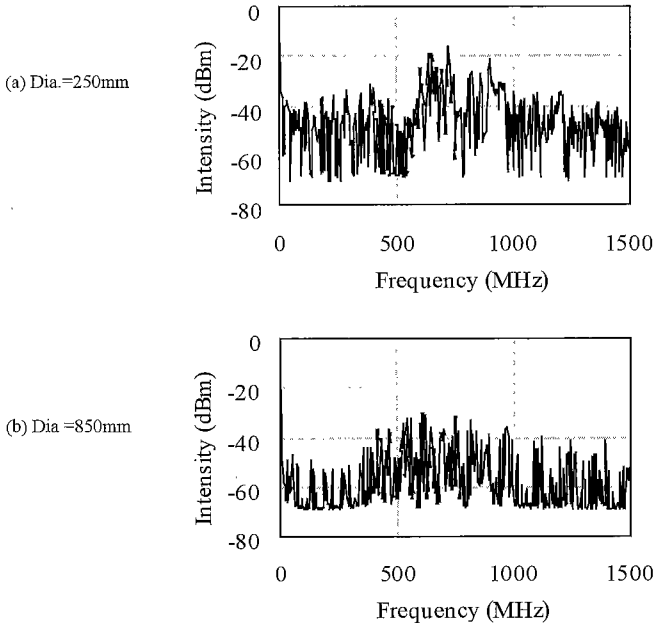

Fig. 10. Intensity from same PD for different tank size

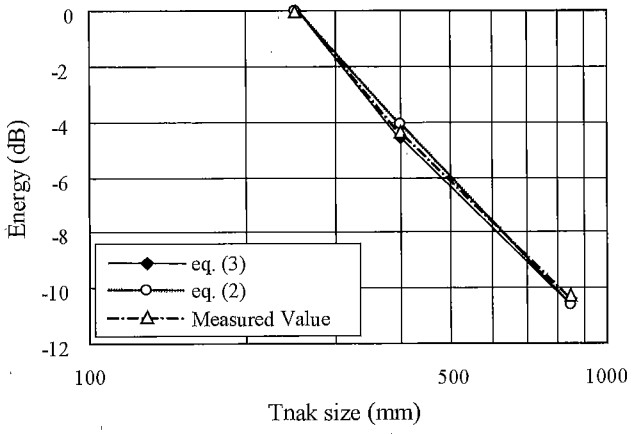

Fig. 11. Discharge energy for different tank sizes

GIS structure is positioned in the coaxial cylinder wave-guide in the environment of an electromagnetic wave. The coaxial cylinder wave-guide is a special form of wave-guide, and three modes of TEM, TE, and TM exist [13)-16)]. Their radial component E_r, and rotational component E_θ in TE_{mn} mode are given by the following equation;

$$\left.\begin{aligned} E_r &= \frac{j\omega\mu mC}{r} Z_m\left(\frac{S'_{mn}r}{b}\right)\sin m\phi e^{\mp jz} \\ E_\theta &= j\omega\mu mCZ'_m\left(\frac{S'_{mn}r}{b}\right)\cos m\phi e^{\mp jz} \end{aligned}\right\} \quad \cdots\cdots(3)$$

where $\omega = 2\pi f$, μ is permeability, $Z_m(x) = AJ_m(x) + BY_m(x)$ in which $J_m(x)$ is the first kind Bessel function, $Y_m(x)$ is the second kind Bessel function of the m'th order, and A, B, and C are constants determined by the boundary conditions. Since the propagation mode generally becomes stronger than the next low mode, evaluation is performed in the TE_{11} mode. Figure 9 shows the electromagnetic distribution E_r in the GIS tank. In this figure, the horizontal axis shows frequency and the vertical axis shows electrical field distribution in the radial and the rotational direction. The electric field is stronger near the conductor than on the tank. As the sensor is usually fitted at the tank wall position, E_r and E_θ are obtained at $r = b$ in eq. (3). E_r is inversely proportional to b and E_θ is independent of b.

Figure 10 shows measured frequency spectra for different tank sizes. Even for the same PD, when tank sizes differ the signal output changes. Figure 11 shows calculated values from the electromagnetic wave analysis by equation (3), the calculated values of apparent charge by equation (2), and measured results. The vertical axis was expressed as dB value for comparison. It is clear that these three lines coincide well with each other. That is, even if the size of real charge is the same, when tank size increases, the apparent charge decreases and the signal output becomes smaller at the same rate. This means that one universal curve is applicable even when different tank sizes are used, as shown in figure 7.

5. Conclusions

UHF PDM system has advantages of high sensitivity and high S/N ratio. Firstly, we clarified the calibration method of the UHF sensor. By injecting the artificial PD pulses of rise time of 0.5 ns, it was confirmed that the same characteristics as actual PDs are acquired. Next, conversion of dBm to pC was investigated experimentally and theoretically to help understanding of severity of PDs. It was clarified that relationship between dBm and pC is independent of different PD sources and tank size, and can be expressed in the universal curve.

(Manuscript received August 27, 2001, revised April 24, 2002)

References

(1) T Kawada, T. Yamagiwa, and F.Endo : "Predictive Maintenance Systems for Substations", *Hitachi Review*, **40**, No.2 (1991)

(2) T Yamagiwa, H. Yamada, F.Endo, Y Oshita, S.Izumi, and I. Yamada : "Development of Preventive Maintenance System for Highly Reliable Gas Insulated Switchgear", *IEEE Trans. Power Delivery*, **6**, No.2, pp.840-848 (1991)

(3) T Yamagiwa and H. Yamada . "Recent Predictive Maintenance Technology for Substation", *T.IEE Japan*, **110-B**, No.5, pp.375-380 (1990-5)

(4) H.Okubo, T.Kato, N.Hayakawa, and M.Hikita : "Temporal Development of Partial Discharge and its Application to Breakdown Prediction in SF_6 Gas", *IEEE Trans. Power Delivery*, **13**, No.2, pp.440-445 (1998)

(5) M.D Judd, O Farish, and B.F.Hampton : "Broadband Couplers for UHF Detection of Partial Discharge in Gas-insulation Substations", *IEE Proc. Science & Measurement Technology*, **142**, No.3 (1995)

(6) J.Girabkenkow, T.Huecker, and U.Schichler "Application of UHF Partial Discharge Monitoring and Expert System Diagnosis", Proc. of 1998 IEEE International Symposium on Electrical Insulation, pp.61-64 (1998)

(7) R Kurrer and K Feser : "The Application of Ultra-High-Frequency Partial Discharge Measurements to Gas-Insulated Substation", *IEEE Trans. Power Delivery*, **13**, No 3, pp 777-782 (1998)

(8) H.Okubo, T.Kato, A.Suzuki, M.Yoshida, N Hayakawa, and M.Hikita : "Voltage Phase Dependence of Partial Discharge Current Pulse Waveform in SF_6 Gas and Its Frequency Characteristics", *T.IEE Japan*, **117-B**, No.1, pp.101-106 (1997-1)

(9) T.Kato, and F.Endo : "Development of UHF Insulation Diagnosis System of GIS", *T.IEE Japan*, **119-B**, No 4, pp.458-463 (1999-4)

(10) N Kock, B.Coric, and R.Pietsch : "UHF PD Detection in Gas-Insulated Switchgear – Suitability and Sensitivity of the UHF Method in Comparison with the IEC 270 Method", *IEEE Electrical Insulation Magazine*, **12**, No.6, pp.20-25 (1996)

(11) CIGRE TF 15/33 03.05 : "Partial Discharge Detention System for GIS: Sensitivity Verification for the UHF Method and the Acoustic Method", ERECTRA, No.183, pp 75-87 (1999)

(12) G C.Crichton, P.W Karlsson, and A.Pedersen . "Partial Discharges in Ellipsoidal and Spheroidal Void", *IEEE. Trans. EI*, **24**, No.2, pp.335-342 (1989)

(13) H.Muto, M.Doi, H.Fujii, and M.Kamei : "Resonance Characteristics and Identification of Modes Electromagnetic Waves Exited by Partial Discharges in GIS", *T.IEE Japan*, **118-B**, No.12, pp.1406-1414 (1998-12)

(14) M.C.Zhang, and H.Li : "TEM- and TE-Mode Waves Excited by Partial Discharge in GIS", Proc of High Voltage Engineering Symposium, No.467, pp.5.144.P5-5.147.P5 (1999)

(15) M.D.Judd, B.F.Hampton, and O.Farish : "Modeling Partial Discharge Excitation of UHF Signals in Waveguide Structure Using Green's Function", *IEE Proc.-Sci. Meas. Technol.*, **143**, No.1, pp.63-70 (1996)

(16) M.D.Judd, O.Farish, and B.F.Hampton : "The Excitation of UHF Signals by Partial Discharge in GIS", *IEEE Trans. Dielectrics & Electrical Insulation*, **3**, No.2, pp.213-228 (1996)

Tatsuro Kato (Member) was born on 11 March, 1969. He received B.S. and Dr. degrees in electrical engineering from Nagoya University, Japan, in 1992 and 1996. He joined Hitachi, Ltd., Japan, in 1996. He has engaged in research of diagnostic system of power apparatus. Now, he is an engineer in Power & Industrial Systems R & D Laboratory, Hitachi, Ltd.

Fumihiro Endo (Member) was born in Tottori, Japan, on 25 November, 1945. He received B.S. and Dr. degrees from Osaka University in 1968 and 1989, respectively. He joined Hitachi Research Laboratory, Hitachi, Ltd., Japan, in 1968, and has been engaged in the research and development of SF_6 gas, air and vacuum insulation, GIS, GCB and diagnostic systems of GIS. Now, he is a chief research engineer in Power & Industrial Systems R & D Laboratory, Hitachi, Ltd. Dr. Endo is members of IEEE and the IEE of Japan.

Shingo Hironaka (Member) was born in Yamaguchi, Japan, on December 17, 1949. He received the B.S degree from Kyusyu Institute of Technology in 1973. He joined Hitachi, Ltd., Kokubu Works, Japan, from 1973 to 1998, and joined Hitachi Engineering & Services., Ltd., Japan from 1998. He has been engaged in the commissioning of Metal-Enclosed Switchgear and diagnosis of substation equipments.